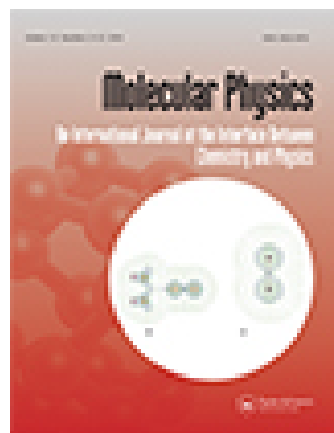


This article was downloaded by: [153.185.48.167]

On: 14 February 2015, At: 14:52

Publisher: Taylor & Francis

Informa Ltd Registered in England and Wales Registered Number: 1072954 Registered office: Mortimer House, 37-41 Mortimer Street, London W1T 3JH, UK



Molecular Physics: An International Journal at the Interface Between Chemistry and Physics

Publication details, including instructions for authors and subscription information:

<http://www.tandfonline.com/loi/tmph20>

Electronic excitation spectra of doublet anion radicals of cyanobenzene and nitrobenzene derivatives: SAC-CI theoretical studies[†]

Hiroyuki Nakashima^a, Yasushi Honda^a, Tadamasa Shida^b & Hiroshi Nakatsuji^a

^a Quantum Chemistry Research Institute (QCRI), JST-CREST, Kyoto, Japan

^b Department of Chemistry, Faculty of Science, Kyoto University, Kyoto, Japan

Published online: 11 Feb 2015.



[Click for updates](#)

To cite this article: Hiroyuki Nakashima, Yasushi Honda, Tadamasa Shida & Hiroshi Nakatsuji (2015): Electronic excitation spectra of doublet anion radicals of cyanobenzene and nitrobenzene derivatives: SAC-CI theoretical studies[†], *Molecular Physics: An International Journal at the Interface Between Chemistry and Physics*, DOI: [10.1080/00268976.2015.1008064](https://doi.org/10.1080/00268976.2015.1008064)

To link to this article: <http://dx.doi.org/10.1080/00268976.2015.1008064>

PLEASE SCROLL DOWN FOR ARTICLE

Taylor & Francis makes every effort to ensure the accuracy of all the information (the "Content") contained in the publications on our platform. However, Taylor & Francis, our agents, and our licensors make no representations or warranties whatsoever as to the accuracy, completeness, or suitability for any purpose of the Content. Any opinions and views expressed in this publication are the opinions and views of the authors, and are not the views of or endorsed by Taylor & Francis. The accuracy of the Content should not be relied upon and should be independently verified with primary sources of information. Taylor and Francis shall not be liable for any losses, actions, claims, proceedings, demands, costs, expenses, damages, and other liabilities whatsoever or howsoever caused arising directly or indirectly in connection with, in relation to or arising out of the use of the Content.

This article may be used for research, teaching, and private study purposes. Any substantial or systematic reproduction, redistribution, reselling, loan, sub-licensing, systematic supply, or distribution in any form to anyone is expressly forbidden. Terms & Conditions of access and use can be found at <http://www.tandfonline.com/page/terms-and-conditions>

RESEARCH ARTICLE

Electronic excitation spectra of doublet anion radicals of cyanobenzene and nitrobenzene derivatives: SAC-CI theoretical studies[†]

Hiroyuki Nakashima^a, Yasushi Honda^{a,‡}, Tadamasa Shida^b and Hiroshi Nakatsuji^{a,*}

^aQuantum Chemistry Research Institute (QCRI), JST-CREST, Kyoto, Japan; ^bDepartment of Chemistry, Faculty of Science, Kyoto University, Kyoto, Japan

(Received 30 November 2014; accepted 10 January 2015)

Electronic ground and excited states of anion radicals of cyanobenzene derivatives: 1,3,5-tricyanobenzene, 1,2,4,5-tetracyanobenzene, and tetracyanoquinodimethane (TCNQ) and nitrobenzene derivatives: nitrobenzene, *p*-nitroaniline, *m*-nitroaniline, and *o*-nitroaniline were theoretically investigated by the symmetry adapted cluster-configuration interaction (SAC-CI) method, which is able to produce accurate theoretical electronic excitation spectra even for radical doublet states. For all the target molecules, the present calculations reproduced the positive electron affinities, which were mostly in good agreement with the experimental values, and their features, especially for TCNQ, were characterised by singly occupied molecular orbitals as well as the number of the electron-withdrawing terminal groups. The excitation energies and their oscillator strengths by the SAC-CI method were also in good agreement with the corresponding experimental UV/VIS/NIR spectra observed by one of the authors and other experimental evidences. Except for TCNQ, the present theoretical calculations were successful to first predict the existences of the forbidden (or very low intense) pure valence excited states in near-infrared region. The physical natures of the observed intense spectral bands were clarified and some new assignments to their electronic states were provided. By extending the present work, photo-related molecular designs of new functional electron acceptors may be challenged.

Keywords: excitation spectrum; anion radical; SAC-CI method; cyanobenzene derivative; nitrobenzene derivative

1. Introduction

Charge-transfer (CT) characters of organic molecular materials have been extensively studied due to their wide-range importance for the molecular technologies such as conductive properties (even superconductivity), molecular memory and switching, photo-induced phase transition, and fluorescence probes in biological phenomena [1–9]. Such CT materials are mostly characterised by the anion radicals of the electron acceptor molecules. In particular, tetracyanoethylene (TCNE) and tetracyanoquinodimethane (TCNQ) are well known as excellent electron acceptors and have been widely studied [2–8,10–18] because both molecules have extremely large positive electron affinities and are easily converted into stable anion radicals [8,12–18]. Furthermore, TCNQ forms unique solid states with remarkably low electrical resistance [4,8] and a photo-induced phase transition in tetrathiafulvalene (TTF)-TCNQ crystals is also well known [5]. Recently, we have proposed an interesting phase-transition mechanism as an alternative to the so-called ‘domino’ mechanism

for its model crystal TTF-TCNE [19]. In addition to the above molecules, 1,3,5-tricyanobenzene (CN3B) and 1,2,4,5-tetracyanobenzene (CN4B) also have large positive electron affinities [12,13,20] and are often associated with electron acceptors. For example, CN4B has been used as an acceptor moiety of CT complexes with 9-methylanthracene for optically anisotropic fluorescent probes [9]. In contrast, the nitro group has a strong electron-withdrawing nature originating from the inductive and resonance effects. The compounds including nitro group, therefore, can also be good candidates for new functional electron acceptors.

In spite of the aforementioned importance, however, the excited states of their anion radicals have not been as thoroughly studied as those of neutral molecules in both experimental and theoretical studies due to their difficult treatments by the instabilities. In gas phase experiments, the electronic structures of anion radicals can be probed with electron transmission spectroscopy (ETS) [21]. However, ETS cannot provide the correct physical assignments to either the states lower than the electron detachment threshold

*Corresponding author. Email: h.nakatsuji@qcri.or.jp

[†]This paper is dedicated to the Late Professor Nicholas Charles Handy for his fundamental achievements in the field of molecular physics and molecular electronic structure theories.

[‡]Present address: West-Japan Office, HPC Systems Inc., 646 Nijohanjikicho, Karasuma-dori-Ayanokoji-sagaru, Shimogyo-ku, Kyoto 600-8412, Japan

or to the states corresponding to the single electron excitation from a doubly occupied molecular orbital to a singly occupied molecular orbital (SOMO). The latter states, which are later assigned to Type II, are associated with a two-electron process from the closed-shell neutral ground state and are called non-Koopmans's states. These states are non-negligible, and rather, are often dominantly important because the actual excitations are only one-electron processes from the open-shell anion ground states. Furthermore, the Koopmans's and non-Koopmans's configurations can interact with each other if they belong to the same symmetry. For instance, Zahradnik and Carsky pointed out the importance of the interaction between the lowest two excited configurations: SOMO-1 to SOMO and SOMO to the lowest unoccupied molecular orbital (LUMO) for an accurate description of the electronic structures for linear conjugated polyene radical ions [22]. This phenomenon is ubiquitous in x-ray photoelectron spectroscopy (XPS), and one can observe weak bands (so-called 'shake-up satellites') next to the main peaks that correspond to the direct electron photodetachments from the inner-shell regions. In the excitation spectra, this phenomenon makes the band assignments difficult and therefore, reliable theoretical tools are required.

On the other hand, one of the authors (T.S.) has developed an experimental method to observe ultraviolet/visible/near-infrared (UV/VIS/NIR) absorption spectra of cation and anion radicals in a transparent glassy solution, where 2-methyltetrahydrofuran (MTHF) was mainly used to stabilise anion radicals [23]. This technique has been applied to the observations of the absorption spectra for hundreds of radical cations and anions since the 1970s. Some spectral data has been interpreted by theoretical analysis using the self-consistent field configuration interaction (SCF-CI) procedure on the basis of Pariser-Parr-Pople (PPP) type approximation about 40 years ago [24–27]. However, only limited numbers of the electronic states were targeted in these theoretical studies, and the accuracy of the calculations was not always satisfactory in view of the recent advances in quantum chemistry.

To perform more reliable theoretical investigations, the symmetry adapted cluster-configuration interaction (SAC-CI) method [28–30] is useful, since it is able to produce accurate theoretical results not only for the ground and ordinary excited states, but also for the ionised and electron-attached states of molecules. Since this method was proposed in 1978, it has been applied to various systems from typical organic materials to metal organic compounds, biological compounds, and surface chemistry [19,31–42]. Whereas most of quantum chemistry methods are not good at accurately describing the excited states of radical species, the SAC-CI method was easily and successfully applied to the excitation spectra of several doublet cation and anion radicals, e.g. benzoquinones [43,44], cyanoethylene and cyanobenzene compounds [45], and unsaturated hy-

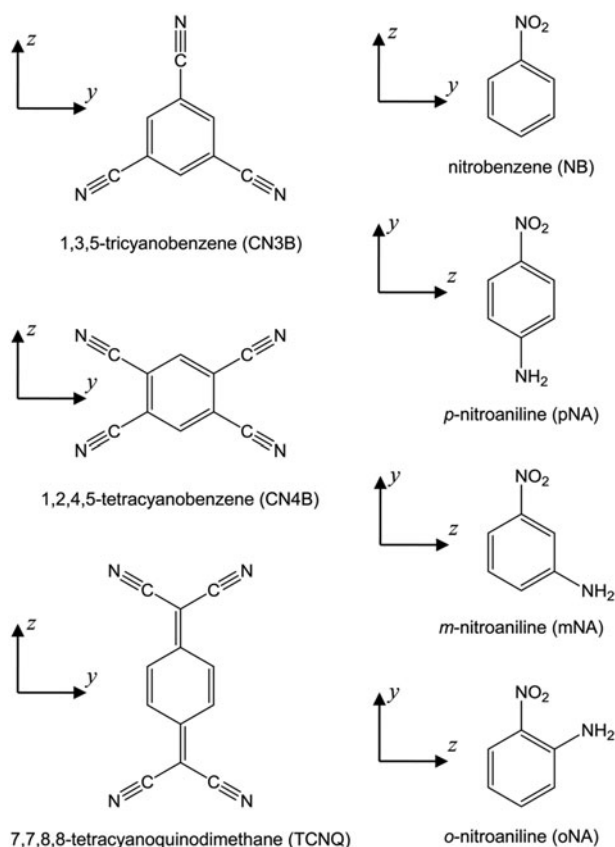


Figure 1. Target anion radicals in the present study.

drocarbons [46]. In the present study, we further systematically investigate the ground and excited states for the anion radicals of the several aforementioned cyanobenzene and nitrobenzene derivatives using the SAC-CI method: 1,3,5-tricyanobenzene (CN3B), 1,2,4,5-tetracyanobenzene (CN4B), tetracyanoquinodimethane (TCNQ), nitrobenzene (NB), *p*-nitroaniline (pNA), *m*-nitroaniline (mNA), and *o*-nitroaniline (oNA), and Figure 1 shows their chemical structures. Connecting the present reliable theoretical results with the corresponding experimental observations would advance our understanding and help to produce further innovations for novel electron acceptors in organic CT materials.

2. Computational method

All the present calculations were carried out using Gaussian 09 program packages [47] where the SAC-CI method is implemented. The molecular geometries of the target anion radicals were optimised by UB3LYP using the D95(d,p) basis set [48] plus Dunning's diffuse anion basis [49] for the carbon, nitrogen, and oxygen atoms. We also optimised the geometries of their neutral molecules to evaluate the vertical and adiabatic electron affinities.

To calculate electronic structures for the anion ground and excited states, we used the SAC-CI singles and doubles (SD-*R*) method, in which one- and two-electron excitation operators were considered as linked operators in the coupled cluster expansion. For the evaluations of electron affinities, the basis set: D95(d,p) + Dunning's diffuse [1s1p] were used. For the theoretical spectra of the anion excited states, D95(d,p) + diffuse [3s3p] ($\alpha(\text{C}) = 0.034, 0.051, 0.068$, $\alpha(\text{N}) = 0.048, 0.072, 0.096$, and $\alpha(\text{O}) = 0.059, 0.0885, 0.118$) were employed. The dependency of the basis sets for the anion excited states was extensively investigated in our previous study [45] and we concluded the triple diffuse functions listed above were significant for accurately describing the excitation spectra of the present anion radicals [45,46]. The 1s orbitals of the carbon, nitrogen, and oxygen atoms were treated as frozen orbitals and excluded from the SAC-CI active space. As reference orbitals for the SAC wave function, we employed the restricted open-shell Hartree-Fock (ROHF) orbitals. Although the restricted Hartree-Fock (RHF) orbitals can be considered as an alternative choice, no significant difference produces in the choice of them according to our previous study [45]. For the linked operators, all of the single excitation operators were employed, and the double excitation operators were selected by the perturbation selection technique [50,51], where the selection threshold: 'LevelThree' ($\lambda_g = 1 \times 10^{-6}$ and $\lambda_e = 1 \times 10^{-7}$) was employed. The perturbation selection can drastically save the computational costs of the SAC-CI calculations for large molecules. We have also examined the adequacy of this threshold with several small anion radicals in our previous study [45] by comparing with the case where all the linked operators are used, and concluded 'LevelThree' is enough. All the unlinked operators were included by the direct algorithm [52] with the keyword 'Direct.' We also employed the group-sum (GSUM) method in the calculation of adiabatic electron affinities to compare the total energies from the different geometries on the perturbation selection technique [45,51,53].

3. Classification of the excited states of anion radicals

To facilitate interpretation of the excited state characters of doublet anion radicals, it is worth to classify the excited states into three excitation types, referred to as Type I, II, and III [43–46], which also correspond to two resonance mechanisms (shape and Feshbach resonances) [54–56]. These electronic configurations are summarised in Figure 2, where M represents a target molecule and M, M^- , M^{2-} , and M^{-*} represent the ground state of neutral molecule, the ground state of anion, the ground state of dianion, and the excited state of anion, respectively.

The main configuration of Type I is represented by an electron promotion from the SOMO to a higher unoccupied orbital. In neutral molecules, since there is no additional

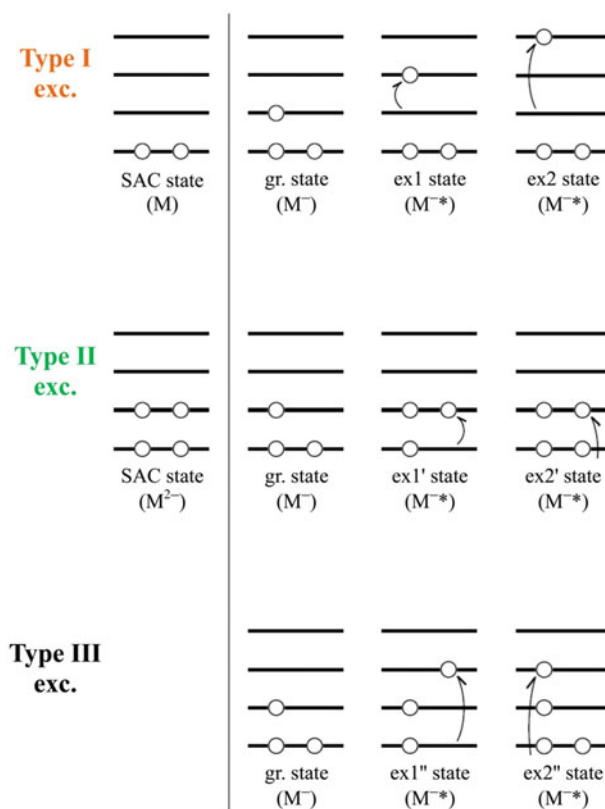


Figure 2. Three-type excitations in the anion radicals. M stands for the target molecule. M, M^- , M^{2-} , and M^{-*} represent the ground state of neutral molecule, the ground state of anion, the ground state of dianion, and the excited state of anion, respectively. White circles represent electrons on the molecular orbitals for target electronic states: the closed-shell neutral and dianion ground (SAC) states, the anion ground (gr.) states, and the anion excited (ex1, ex2, ex1', ex2', ...) states.

electron in SOMO, the corresponding excited states to Type I do not exist. Type I excitations, therefore, are specific for anions. Such states can be described as one-electron attachment to neutral molecules. In the SAC-CI method, these states can be evaluated as one-electron process by the keyword 'AnionDoublet' from the closed-shell ground (SAC) state of neutral molecule. The Type I states include not only the excited states with valence characters but also a lot of diffuse and/or Rydberg states. Although we are mainly interested in the valence excited states, diffuse basis functions cannot be negligible [45] to correctly describe the valence-Rydberg state separations [57].

The main configuration of Type II is represented by an electron promotion from a doubly occupied orbital to the SOMO. In contrast to the Type I case, the corresponding excitations to Type II exist in neutral molecules. Such states can be described as one-electron detachment from dianion. In the SAC-CI method, these states can be also evaluated as one-electron process by the keyword 'CationDoublet' from the closed-shell ground (SAC) state of dianion. In

contrast to Type I, all the Type II excited states have valence characters since an electron motion always occur among valence orbitals. Diffuse basis functions, therefore, are not very significant, compared to the case of Type I.

Type III is mainly represented by an electron promotion from a doubly occupied orbital to an unoccupied orbital beyond the SOMO. Thus, Type III cannot be expressed by any one-electron process from closed-shell configuration. Whereas the Type I and II excited states can be easily calculated by the SAC-CI SD-*R* method with the aforementioned keywords, the SAC-CI general-*R* method [58,59] is required for the accurate calculations of Type III. However, the Type III excited states are expected to have higher excitation energies than the energy region where we are interested ($< \sim 5$ eV), and we considered only the Type I and II excited states with the SAC-CI SD-*R* method in the present work.

When the excited states of anion radicals lie above its electron detachment threshold or the energies of neutral molecule, they are observed as resonance states with finite lifetimes (femto second and pico second scale, in general). As seen from Figure 2, since the detachment from a Type I excited state gives the ground state of neutral molecule, the Type I excited states above the detachment threshold induce a shape resonance character. On the other hand, the detachment from a Type II state produce an excited state of neutral molecule and it induces a Feshbach resonance [45].

4. Optimised geometries of the target anion radicals and their neutral states

First, we performed the geometry optimisations for the ground states of both anion and neutral molecules. The resultant optimised geometries of the CN3B, CN4B, and TCNQ anions were planar and have the symmetries with D_{3h} , D_{2h} , and D_{2h} , respectively, same as in the neutral molecules. The optimised geometry of the NB anion was also planar in consistent with the experimental results both in solution [60] and in crystal [61]. On the other hand, pNA, mNA, and oNA anions were not strictly planar structures due to the existences of the sp^3 -hybrid $-NH_2$ groups: two hydrogen atoms deviated from the planar. For these non-planar molecules, although the π and σ symmetries mix each other and cannot be definitely distinguished, we approximately use the terms of ' π ' and ' σ ' for simple and intuitive understandings in all the discussions below. Their mixing, however, is sometimes essential and non-negligible to explain the electronic structures. The optimised geometries of the neutral molecules of NB, pNA, and mNA were similar to their anion radicals. The neutral molecule of oNA, however, was planar, different from its anion radical. In neutral oNA, the single hydrogen atom in $-NH_2$ group formed a hydrogen bond with the oxygen in $-NO_2$ group and $-NH_2$ group that weakly participated in the π conjugation of the benzene ring. A planar structure, therefore, is rather

favourable for neutral oNA. This phenomenon, however, does not occur in the anion radical since the π conjugation of $-NH_2$ group cannot be created due to the existence of the additional electron. It also does not occur in mNA and pNA since the hydrogen bond between $-NO_2$ and $-NH_2$ groups cannot be formed due to their long distance.

In the SAC-CI calculations of the anion radicals, we used these optimised geometries and imposed the symmetry option of the abelian group except for mNA and oNA to reduce computational costs, i.e. C_{2v} , D_{2h} , D_{2h} , C_{2v} , C_s , C_1 , and C_1 were employed for CN3B, CN4B, TCNQ, NB, pNA, mNA, and oNA, respectively.

5. Electron affinities

On the optimised geometries of anion and neutral molecules, the vertical and adiabatic electron affinities (EA) were calculated by the SAC-CI method and Table 1 summarises their results together with the corresponding experimental values [12–16,20,62–68]. The calculated EAs showed good agreement with the experimental values and they were positive for all the molecules in Table 1, i.e. all the target anion radicals were more stable than their respective neutral molecules. This outcome is due to the electrophilic character of the benzene moiety caused by the strong electron-withdrawing groups, $-CN$ and $-NO_2$.

The calculated adiabatic EAs of CN3B and CN4B were 1.41 and 2.19 eV, respectively. On the other hand, those for (mono)cyanobenzene (CNB) and dicyanobenzenes (CN2B; *o*-, *m*-, and *p*-isomers) were reported to be 0.063 and 1.20–1.26 eV [69,70], respectively, and, therefore, $EA(CN4B) > EA(CN3B) > EA(CN2B) > EA(CNB)$. The $-CN$ electron-withdrawing strengths account for this outcome and are consistent with the experimental trends [12,13,20]. Interestingly, the adiabatic EA of TCNQ was very large (3.31 eV in our calculations and 2.80–2.88 eV in the experiments [12–16]) as compared to CN4B in spite of having the same number of the $-CN$ groups. This result can be attributed to the SOMO for each anion radical (or the lowest unoccupied molecular orbital (LUMO) for each neutral molecule) and a conjugation effect. Figure 3 shows SOMOs (LUMOs) and bond lengths for CN4B and TCNQ anion/neutral molecules. For comparison, the data for 1,1,2,2-tetracyanoethylene (TCNE) are also shown. For neutral CN4B, the CC bond lengths of the benzene ring were calculated to be 1.403 and 1.418 Å, which were quite similar to those of the benzene molecule. The SOMO has anti-bonding natures on a part of the CC bonds, and electron accommodation to the SOMO caused deviations from the regular hexagonal structure of the ring in the anion. Indeed, the anti-bonding CC bonds for CN4B anion were elongated to 1.463 Å whereas the other CC bond lengths were not changed in our calculations. Therefore, the conjugation effect would become smaller and the stabilisation due to the electron attachment would be diminished. On

Table 1. Theoretical and experimental electron affinities (EA).

Molecules ^a	EA types ^b	Electron affinities (eV)	
		SAC-CI	Exptl.
1,3,5-tricyanobenzene (CN3B)	Vertical (Neutral)	1.18	
	Vertical (Anion)	1.48	1.84 ^c
	Adiabatic	1.41	1.5 ^c
1,2,4,6-tetracyanobenzene (CN4B)	Vertical (Neutral)	2.19	
	Vertical (Anion)	2.45	
	Adiabatic	2.19	2.15 ^d , 2.21 ^e
Tetracyanoquinodimethane (TCNQ)	Vertical (Neutral)	3.25	
	Vertical (Anion)	3.56	
	Adiabatic	3.31	2.88 ^d , 2.83 ^e , 2.80 ^f
Nitrobenzene (NB)	Vertical (Neutral)	0.40	
	Vertical (Anion)	1.08	1.18 ^g
	Adiabatic	0.63	1.00~1.0 ^{g,h,i}
p-nitroaniline (pNA)	Vertical (Neutral)	0.90	
	Vertical (Anion)	0.94	
	Adiabatic	0.86	0.92 ^j
m-nitroaniline (mNA)	Vertical (Neutral)	0.40	
	Vertical (Anion)	1.16	
	Adiabatic	0.38	0.95 ^h

The definite EAs were not be able to be obtained for oNA owing to problems on non-negligible dependence of the energies with the perturbation selection upon the molecular geometry and absence of experimental data for comparison.

'Vertical (Neutral)', 'Vertical (Anion)', and 'Adiabatic' stand for the vertical EA at the neutral geometry, the vertical EA at the anion geometry, and the adiabatic EA, respectively.

Ref. [20].

Ref. [12].

Ref. [13].

Ref. [14–16].

Ref. [62].

Ref. [63].

Ref. [64–67].

Ref. [68].

the other hand, the SOMO for TCNQ had bonding and anti-bonding natures on the single and double CC bonds, respectively, making the C-C and C = C bond lengths similar to each other. Consequently, the conjugation effect for the TCNQ anion became larger than the neutral form, and the stabilisation energy of the anion would be enhanced. This outcome is consistent with the reported discussion using HF/6-31G* calculations [17]. Furthermore, this trend is more pronounced for TCNE, which had an extremely large adiabatic EA, 3.68 eV in our previous calculations [45] and 3.17 ± 0.2 eV in the experimental data [70]. The SOMO for TCNE also had bonding and anti-bonding amplitudes on the single and multiple CC bonds, respectively. When an electron is attached to the SOMO, the C = C bond became elongated from 1.376 to 1.444 Å, whereas the C-C bonds would shorten from 1.435 to 1.418 Å, resulting in significant bond alternation. Thus, the EA order (CN4B < TCNQ < TCNE) can be attributed to the conjugation effects.

For NB, pNA, and mNA, the experimental and calculated vertical EAs at the anion geometries are similar to each other. This is due to the small MO amplitudes of SOMOs (LUMOs for the neutral molecules) on the -NH₂ groups. Since the anion ground states of these molecules are substantially described by the electron promotion to the

SOMOs, the stabilisation effects are expected to be less sensitive to the -NH₂ groups. The lesser agreement between the calculated and experimental adiabatic EAs for mNA can be associated with balancing among the different geometries caused by the perturbation selection technique and larger configuration space should be required for improvement. Unfortunately, the definite EAs for oNA were not able to be obtained owing to the same problem and no experimental data was also available in the literature as long as we know.

6. Electronic excitation spectra of anion radicals

Let us start the discussions of the theoretical excitation spectra of the anion radicals by the SAC-CI method, compared with the experimental observations. As a general tendency, most unoccupied orbitals have diffuse characters and their corresponding excited states belonging to Type I also display diffuse natures. Although the assignments of such states are not straightforward due to large mixing between valence and diffuse characters, we used the second moments to provide correct assignments with distinguishing such mixing excited states. In the discussion below, we will refer to the π^* SOMO as ' $\pi^*(s)$ ' and the diffuse-mixed

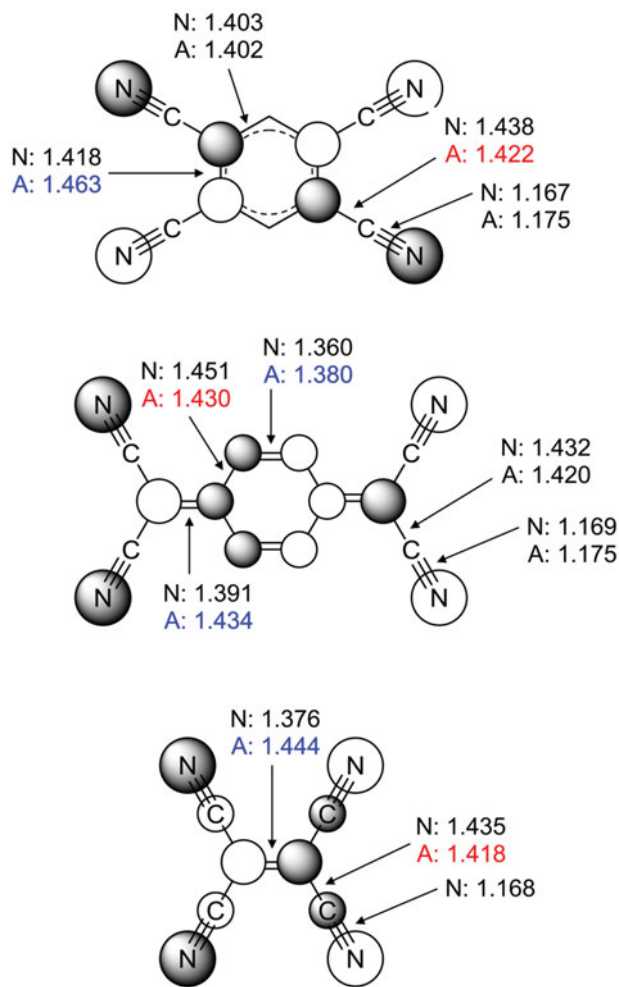


Figure 3. SOMO for CN4B, TCNQ, and TCNE together with their bond lengths. The white and shaded circles on the atoms stand for π orbitals with opposite phase to each other. Values with N and A are bond lengths (in Å) for the neutral and anion molecules, respectively. Data for TCNE were taken from Ref. [45]. The red and blue fonts mean that the bond length of the anion is smaller and larger than that of the neutral molecule, respectively.

π^* and σ^* characters of the anion states as ' π^* ' and ' σ^* ', respectively, for simplicity. On the other hand, valence π^* and σ^* characters (with small diffuse characters) will be specifically represented as ' $\nu\pi^*$ ' and ' $\nu\sigma^*$ ', respectively.

Natures, excitation energies, and oscillator strengths of the electronic ground and some remarkable excited states for the anion radicals are summarised in Tables 2 and 3 for the cyanobenzene and nitrobenzene derivatives, respectively, together with the experimental results available in the literatures. All the calculated electronic states including pure diffuse excitations are summarised in the supplemental tables (Tables S1–S7). Figures 4 and 5 show the theoretical (this work) and experimental [23] excitation spectra for the cyanobenzene and nitrobenzene derivatives, respectively. All the theoretical calculations were performed in the gas phase, whereas the experimental spectra were

Table 2. Nature of the electronic state, excitation energy ΔE (eV), and oscillator strength f of the electronic ground and some remarkable excited states ($\Delta E < \sim 5.0$ eV) of cyanobenzene anion radicals.

1,3,5-tricyanobenzene (CN3B)				1,2,4,5-tetracyanobenzene (CN4B)				tetracyanoquinodimethane (TCNQ)					
SAC-CI	Nature & excitation type	ΔE	f	SAC-CI	Nature & excitation type	ΔE	f	SAC-CI	Nature & excitation type	State	ΔE	f	Exptl.
X^2B_1	(ground st.)	—	—	X^2A_u	(ground st.)	—	—	X^2B_{2g}	(ground st.)	X^2B_{2g}	—	—	—
1^2A_2	$\pi^*(s)\nu\pi^*(l)$	0.30	0.000	1^2B_{3u}	$\pi^*(s)\nu\pi^*(l)$	$\sim 0.6^a$	fb	1^2B_{3u}	$\pi^*(s)\nu\pi^*(l)$	1^2B_{3u}	1.79	0.675	1.44 ^a , 1.5 ^f , 1.48 ^g
1^2B_1	$\pi^*(s)\nu\pi^*(l)$	2.07	0.018	1^2B_{2g}	$\pi^*(s)\nu\pi^*(l)$	3.15	0.334	2^2B_{3u}	$\pi^*(s)\nu\pi^*(l)$	2^2B_{3u}	3.19	0.312	$\sim 2.9^a, 3.1^f, 3.14^g, \sim 2.8^h$
3^2B_1	$\pi^*(s)\nu\pi^*(l)$	2.91	0.210	3^2A_g	$\pi^*(s)\nu\sigma^*(l)$	3.51	fb	1^2A_u	$\pi^*(s)\nu\pi^*(l)$	1^2A_u	3.26	0.025	$\sim 3.5^h, 3.2^i$
4^2B_1	$\pi^*(s)\nu\pi^*(l)$	3.59	0.022	2^2B_{2g}	$\pi^*(s)\nu\pi^*(l)$	3.68	0.090	1^2B_{2u}	$\pi^*(s)\nu\pi^*(l)$	1^2B_{2u}	4.13	fb	4.0 ⁱ
3^2A_2	$\pi^*(s)\nu\pi^*(l)$	3.62	0.017	1^2B_{1g}	$\pi^*(s)\nu\pi^*(l)$	3.79	0.224	3^2B_{3u}	$\pi^*(s)\nu\pi^*(l)$	3^2B_{3u}	4.27	0.015	$\sim 4.1^h, 4.2^i$
6^2B_1	$\pi^*(s)\nu\pi^*(l)$	4.15	0.134	2^2B_{1u}	$\pi^*(s)\nu\sigma^*(l)$	4.12	fb	2^2B_{1g}	$\pi^*(s)\nu\pi^*(l)$	2^2B_{1g}	4.96	fb	4.9 ⁱ
7^2B_2	$\pi^*(s)\nu\sigma^*(l)$	4.34	fb ^b	3^2B_{2g}	$\pi^*(s)\nu\pi^*(l)$	4.45	0.114						
				3^2B_{1g}	$\pi^*(s)\nu\pi^*(l)$	5.10	0.092						

Ref. [23] (in MTHF).

fb, forbidden. The same notation is employed in all the tables including supplemental information.

Ref. [71] (in poly (vinyl alcohol) film after irradiation with 330 MeV Ar^{1+} ions).

Ref. [72] (in poly(N-vinylcarbazole) films doped with tetramethyl-p-phenylenediamine).

Ref. [73] (in electron-donating zeolites).

Ref. [16] (gas-phase).

Ref.[10] (K^+TCNQ^- in acetonitrile solution).

Ref. [15] (gas-phase). The excitation energies from the neutral ground state in the literature are converted to those from the anion ground state in this table, assuming that the adiabatic EA is 2.8 eV.

Ref. [11] (gas-phase). The values of the excitation energies are converted as with the footnote h, assuming that the adiabatic EA is 2.8 eV.

Table 3. Nature of the electronic state, excitation energy ΔE (eV), and oscillator strength f of the electronic ground and some remarkable excited states ($\Delta E < \sim 5.0$ eV) of nitrobenzene anion radicals.

nitrobenzene (NB)			<i>p</i> -nitroaniline (pNA)			<i>m</i> -nitroaniline (mNA)			<i>o</i> -nitroaniline (oNA)		
SAC-CI	Nature & excitation type	Exptl.	SAC-CI	Nature & excitation type	Exptl.	SAC-CI	Nature & excitation type	Exptl.	SAC-CI	Nature & excitation type	Exptl.
	ΔE	f	ΔE	f	ΔE	ΔE	f	ΔE	ΔE	f	ΔE
X^2B_1	(ground st.)	—	X^2A'	(ground st.)	—	X^2A	(ground st.)	—	X^2A	(ground st.)	—
1^2A_2	$\pi^*(s)\text{-}v\pi^*(I)$	1.95 0.005	$2^2A'$	$\pi^*(s)\text{-}v\pi^*(I)$	1.54 0.004	4^2A	$\pi^*(s)\text{-}v\pi^*(I)$	1.91 0.003	3^2A	$\pi^*(s)\text{-}v\sigma^*(I)$	1.83 0.011
2^2B_1	$\pi^*(s)\text{-}v\pi^*(I)$	2.65 0.264	$3^2A'$	$\pi^*(s)\text{-}\pi^*(I)$	1.74 0.020	5^2A	$\pi^*(s)\text{-}v\pi^*(I)$	2.16 0.051	5^2A	$\pi^*(s)\text{-}\pi^*(I)$	2.14 0.026
3^2B_2	$n\text{-}\pi^*(s)(II)$	3.00 fb	$5^2A'$	$\pi^*(s)\text{-}v\pi^*(I)$	2.35 0.099	8^2A	$\pi^*(s)\text{-}v\pi^*(I)$	2.51 0.157	7^2A	$\pi^*(s)\text{-}\sigma^*(I)$	2.44 0.050
4^2B_1	$\pi^*(s)\text{-}\pi^*(I)$	3.58 0.026	$7^2A'$	$\pi^*(s)\text{-}v\pi^*(I)$	2.75 0.095	11^2A	$\pi^*(s)\text{-}\pi^*(I)$	2.89 0.038	8^2A	$\pi^*(s)\text{-}v\pi^*(I)$	2.46 0.112
4^2A_2	$\pi\text{-}\pi^*(s)(II)$	3.66 0.093	$9^2A'$	$\pi^*(s)\text{-}\pi^*(I)$	3.24 0.025	12^2A	$n\text{-}\pi^*(s)(II)$	3.01 0.000	11^2A	$\pi^*(s)\text{-}\pi^*(I)$	2.85 0.017
7^2A_1	$n\text{-}\pi^*(s)(II)$	3.86 0.000	$6^2A'$	$n\text{-}\pi^*(s)(II)$	3.23 0.000	17^2A	$\pi\text{-}\pi^*(s)(II)$	3.65 0.076	14^2A	$n\text{-}\pi^*(s)(II)$	3.32 0.000
6^2B_1	$\pi^*(s)\text{-}\pi^*(I)$	4.60 0.006	$9^2A'$	$\pi\text{-}\pi^*(s)(II)$	3.82 0.097	21^2A	$n\text{-}\pi^*(s)(II)$	3.88 0.000	16^2A	$\pi^*(s)\text{-}\pi^*(I)$	3.61 0.009
7^2B_1	$\pi\text{-}\pi^*(s)(II)$	4.80 0.112	$15^2A'$	$n\text{-}\pi^*(s)(II)$	4.06 0.000	27^2A	$\pi\text{-}\pi^*(s)(II)$	4.60 0.092	19^2A	$\pi\text{-}\pi^*(s)(II)$	3.96 0.102
			$18^2A'$	$\pi\text{-}\pi^*(s)(II)$	4.72 0.107	28^2A	$\pi\text{-}\pi^*(s)(II)$	5.19 0.053	22^2A	$n\text{-}\pi^*(s)(II)$	4.21 0.002
									27^2A	$\pi\text{-}\pi^*(s)(II)$	4.59 0.061

Ref. [23] (in MTHF).

Ref. [62] (gas-phase).

Ref. [74] (gas-phase). The excitation energies from the neutral ground state in the literature are converted to those from the anion ground state in this table, assuming that the adiabatic EA is 1.0 eV. Tentative assignments.

observed in the MTHF matrix [23]. Environmental effects of the MTHF matrix for the excitation spectra, however, would be not serious since the randomly oriented MTHF matrix is frozen and immobile at 77 K and the dielectric effects to the anion radicals are almost same among the ground and excited states. Therefore, the direct comparisons between the theoretical and experimental spectra under the present condition should be reasonable. In the following discussion, we provide the theoretical explanations to understand the electronic structures of the excited states with their reliable assignments to the experimental peaks.

6.1. Cyanobenzene derivatives

6.1.1. CN3B and CN4B

In the excited states of the CN3B and CN4B anions, we first notice the existences of the pure valence excited states $\pi^*(s)\text{-}v\pi^*$ (Type I) in near-infrared region at 0.30 and 0.96 eV corresponding to the 1^2A_2 and 1^2B_{3u} states, respectively. These electronic states have complete bound characters because they locate notably lower energy than the electron detachment threshold (see the vertical EAs of anions in Table 1). These delocalised valence π^* orbitals derive from the resonance effect of the benzene ring. Although the electron excitations to these states are forbidden transitions at the D_{3h} and D_{2h} symmetries in CN3B and CN4B, respectively, a very weak band at ~ 5000 cm^{-1} (~ 0.6 eV) was observed in the experimental spectra of the CN3B anion. This is due to a symmetry violation of the Jahn–Teller effect. On the other hand, in the CN4B anion, no peak was detected in near-infrared region in the experimental spectra. Thus, this hidden valence state was first theoretically predicted in the present work. This situation was same as in our previous study of the *p*-cyanobenzene anion [45]. In that case, after the careful reexamination of the experimental spectrum, the $\pi^*(s)\text{-}v\pi^*$ bound state was confirmed to be real. From both the present and previous studies [45], we can conclude that the anion radicals of highly symmetric cyanobenzene derivatives always have a low-energy hidden $\pi^*(s)\text{-}v\pi^*$ (Type I) excited state with very weak intensity in common. In the TCNQ anion, on the other hand, the corresponding excited state does not exist in low energy region since the $\pi^*\text{-}\pi^*$ gap is larger than the CN3B and CN4B cases due to the lack of the resonance effect as appeared in the benzene π ring.

In the experimental excitation spectra of the CN3B and CN4B anions, the first intense bands at 542 nm (2.29 eV) and 462 nm (2.68 eV) were assigned to the $\pi^*(s)\text{-}v\pi^*$ (Type I) states at 2.91 and 3.15 eV corresponding to the 1^2A_2 and 1^2B_{3u} states, respectively, in the theoretical spectra. The second intense bands at 3.63 and 4.43 eV in the experimental spectra were assigned to the 6^2B_1 and 3^2B_{2g} : $\pi\text{-}\pi^*(s)$ (Type II) states in the CN3B and CN4B anions, respectively. Our calculations also predict the other forbidden

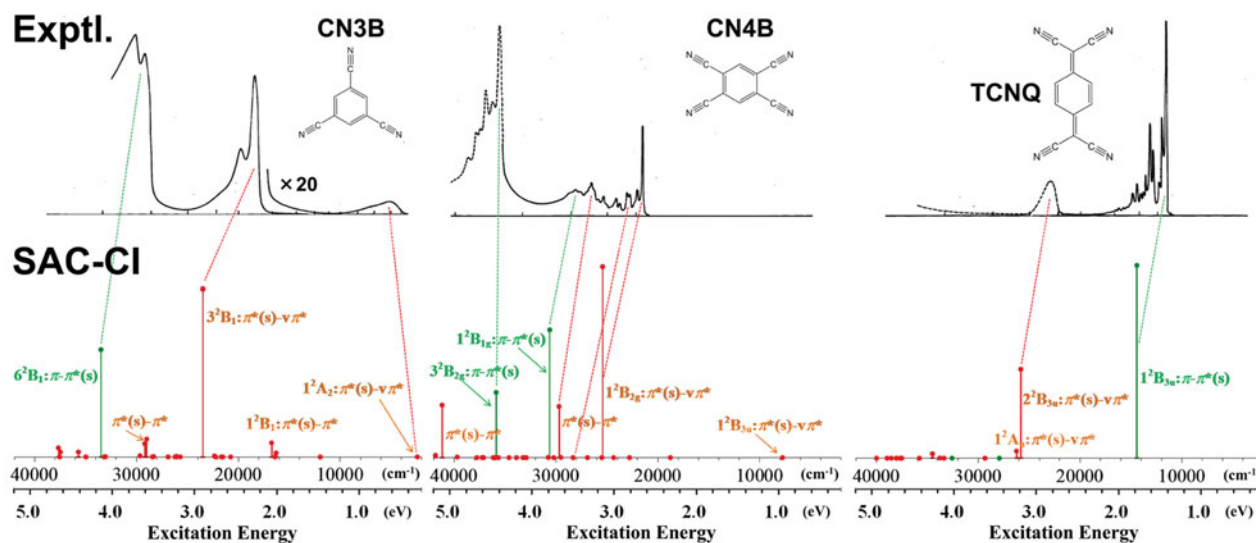


Figure 4. Excitation spectra (horizontal axis: excitation energy and vertical axis: relative oscillator strength) of the anion radicals of the cyanobenzene derivatives (CN3B, CN4B, and TCNQ) by the SAC-CI method (lower) and as observed experimentally (upper) [23]. In the SAC-CI spectra, the red circle and line represent Type I excitation and the green ones show Type II excitation. The natures of the excited states and our theoretical assignments to the experimental peaks are also given.

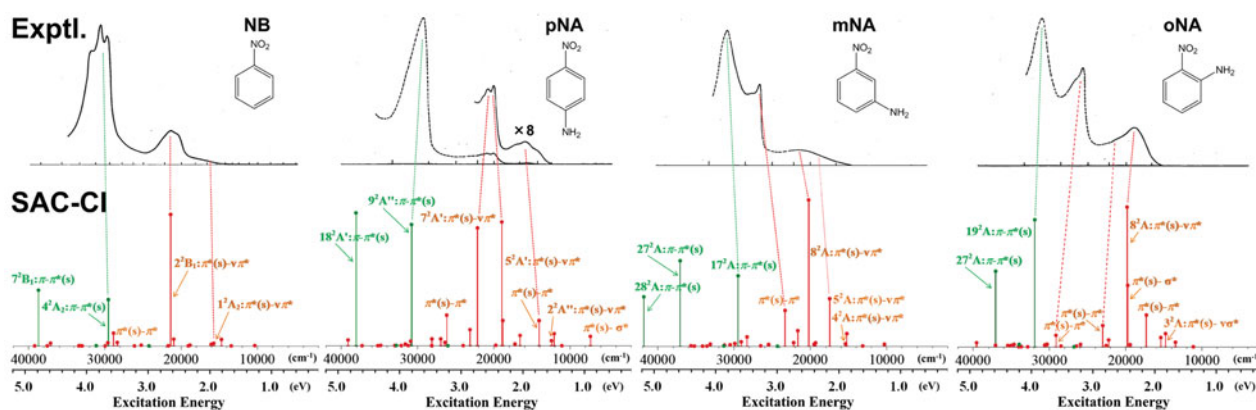


Figure 5. Excitation spectra (horizontal axis: excitation energy and vertical axis: relative oscillator strength) of the anion radicals of the nitrobenzene derivatives (NB, pNA, mNA, and oNA) by the SAC-CI method (lower) and as observed experimentally (upper) [23]. In the SAC-CI spectra, the red circle and line represent Type I excitation and the green ones show Type II excitation. The natures of the excited states and our theoretical assignments to the experimental peaks are also given.

valence excited states at 4.34 and 4.12 eV, assigned to the 7^2B_2 and $2^2B_{1u}:\pi^*(s)-v\sigma^*$ (Type I) states.

In the CN3B anion, besides the above valence electron excitations, three states with weak intensities were also calculated at 2.07 (1^2B_1), 3.59 (4^2B_1) and 3.62 eV (3^2A_2), assigned to $\pi^*(s)-\pi^*$ having diffuse characters. In the CN4B anion, we also observed a series of the complicated peaks at 22,000–30,000 cm^{-1} in the experimental spectrum and, correspondingly, several electronic states were identified in our calculations. To suggest the assignments for these peaks, we compared the theoretical spectrum to other experimental studies [71–73]. Measurements by Taguchi et al. [71] were closely related to our investigations. They observed absorption spectra of poly (vinyl alcohol) film

doped with CN4B after irradiation with 330 MeV Ar^{11+} ions. The absorption bands observed in the 340–480 nm (2.5–3.7 eV) region after the irradiation were ascribed to the CN4B anion radical. In their spectrum, three peaks were observed at 464 nm (2.67 eV), 438 nm (2.83 eV), and 377 nm (3.29 eV). These peaks were expected to correspond to those at 462 nm (2.68 eV), 433 nm (2.86 eV), and 377 nm (3.29 eV) in the experimental spectrum in Figure 4. Furthermore, we recognised a slight and broad absorption band at ~ 350 nm in the spectrum of Taguchi et al. and this band can be associated with the peak at 353 nm (3.51 eV) in Figure 4. Thus, we concluded that there are four electronic states, at least, at the 20,000–30,000 cm^{-1} (2.5–3.7 eV) region, besides the vibrational structures. We assigned the

states at ~ 2.86 , 3.29 , and 3.51 eV to $3^2A_g: \pi^*(s)-v\sigma^*$, $2^2B_{2g}: \pi^*(s)-\pi^*$, and $1^2B_{1g}: \pi-\pi^*(s)$, respectively, judging from the oscillator strengths and second moments.

6.1.2. TCNQ

Since TCNQ is one of the most important and stable electron acceptors used in the material science, many experimental studies are available about the excited states of the TCNQ anion [10,11,15,16,23]. Two intense peaks at $11,600\text{ cm}^{-1}$ (1.44 eV) and $\sim 23,000\text{ cm}^{-1}$ (~ 2.9 eV) were observed in the experimental spectrum and they were assigned to the $1^2B_{3u}: \pi-\pi^*(s)$ (Type II) and $2^2B_{3u}: \pi^*(s)-v\pi^*$ (Type I) states at 1.79 and 3.19 eV, respectively. Thus, the former lowest excited state of the TCNQ anion is Type II $\pi-\pi^*(s)$, distinct from the other target anion radicals, for which Type I excited states were the lowest. This observation was due to the large EA, in other words, the greater stability of the SOMO of TCNQ, as discussed in Section 5. The lowered energy of the SOMO causes blue- and redshifts of the Type I and Type II excitation energies, respectively. The same phenomenon was noted for TCNE with a very large EA, as reported in our previous study [45]. Since these states are lower than the vertical EA of anion (3.56 eV), both the 1^2B_{3u} (1.79 eV) and 2^2B_{3u} (3.19 eV) states are considered as complete bound states. In our calculations, no electronic states were found between 1^2B_{3u} and 2^2B_{3u} , and this situation was not changed even after more accurate calculations with larger basis set. Therefore, many peaks at the $11,000$ – $17,000\text{ cm}^{-1}$ region in the experimental spectrum can be attributed to the vibrational structures of the 1^2B_{3u} state. In the other experimental studies, Iida reported electronic spectroscopy of K^+TCNQ^- in acetonitrile solution and observed absorption peaks at $11,900\text{ cm}^{-1}$ (1.48 eV) and $25,300\text{ cm}^{-1}$ (3.14 eV) [10]. Brinkman et al. observed electronic states at $\sim 825\text{ nm}$ (1.5 eV) and $\sim 400\text{ nm}$ (3.1 eV) by photodetachment spectroscopy [16]. For both observations, the lower and higher bands could be assigned to the 1^2B_{3u} and 2^2B_{3u} states, respectively. The second lowest peaks at $\sim 13,000\text{ cm}^{-1}$ in Ref. [10] and at 770 nm in Ref. [16] are assigned to the vibrational bands of the 1^2B_{3u} state.

In the electronic spectra in Figure 4, there is almost no information about the higher electronic states above the 2^2B_{3u} state. Some other experimental researchers, however, reported about such higher electronic states. Compton and Cooper observed several electronic excited states of the TCNQ anion as well as the EA measurements using gas-phase collisions of electron and fast cesium beam with TCNQ [15]. They reported metastable states with respect to the electron autodetachment at ~ 0 , 0.7 , and 1.3 eV above the detachment threshold. Assuming that the adiabatic EA is 2.8 eV, the common experimental values reported by several research groups in addition to Compton and

Cooper [15], these energies are translated to ~ 2.8 , 3.5 , and 4.1 eV from the anion ground state, respectively. We assigned these states to three Type I excited states, $2^2B_{3u}: \pi^*(s)-v\pi^*$, $1^2A_u: \pi^*(s)-v\pi^*$, and $3^2B_{3u}: \pi^*(s)-\pi^*$ at 3.19 , 3.26 , and 4.27 eV, respectively. The energy position of the second one at 3.5 eV is closer to that of our theoretical result $1^2B_{1g}: \pi-\pi^*(s)$ (3.46 eV) rather than $1^2A_u: \pi^*(s)-v\pi^*$ (3.26 eV). However, the 1^2B_{1g} state belongs to Type II, and we do not think that the electron collision to the ground-state TCNQ is likely to provide Type II states. Therefore, we proposed the above assignments. On the other hand, Burrow et al. [11] reported ETS experiments of several cyano compounds and observed excited states of the TCNQ anion at 0.35 , 1.22 , 1.40 , and 2.12 eV above the electron detachment threshold, which correspond to ~ 3.2 , 4.0 , 4.2 , and 4.9 eV from the anion ground state, respectively, assuming that the adiabatic EA is 2.8 eV. They gave their own assignments to these states based on the HF/3-21G calculation of TCNQ. Although they assigned the state at 0.35 eV (~ 3.2 eV in our definition) to 2^2A_u in accordance with our interpretation, the assignments of the other states differed from ours. We think that this discrepancy is due to the lack of both basis set space and electron correlation effects in their HF/3-21G calculation.

Thus, our theoretical results for the remarkable electronic states were very good agreement with many experimental evidences. It shows that the SAC-CI theoretical calculations are reliably used in the material designs related to the TCNQ derivatives.

6.2. Nitrobenzene derivatives (NB, pNA, mNA, and oNA)

In the excited states of the NB, pNA, and mNA anions, our calculations predicted the pure valence excited states $\pi^*(s)-v\pi^*$ (Type I) in lower energy region at 1.95 , 1.54 , and 1.91 eV corresponding to the 1^2A_2 , $3^2A'$, and 4^2A states, respectively. They can be found as the shoulders of the lowest peak in the experimental spectra. These states derive from the same origins but with a little higher energies as shown in the CN3B and CN4B anions. However, different from the CN3B and CN4B cases, they are not considered as bound states since their excitation energies are higher than the vertical EAs of anions. In the NB anion, the large and small peaks at 2.36 and 1.7 eV were assigned to the 2^2B_1 and $1^2A_2: \pi^*(s)-v\pi^*$ states, respectively, judging from their relatively small second moment. These states correspond to those at 2.67 and ~ 2.0 eV observed in an earlier study in Ref. [23]. In the pNA anion, the weak band around $16,000\text{ cm}^{-1}$ (~ 2.0 eV) in the spectrum was assigned to the $3^2A': \pi^*(s)-\pi^*$ state, and the somewhat intense band at ca. $20,000$ – $22,000\text{ cm}^{-1}$ (2.5 – 2.7 eV) was assigned to the two Type I $\pi^*(s)-v\pi^*$ states of $5^2A'$ and $7^2A'$, considering the excitation energies, oscillator strengths, and second moments. The assignment to $3^2A'$ is based on the

excitation energy and intensity rather than the second moment. Similarly, in the mNA, the lower broad band at 16,000–21,000 cm^{-1} (2.0–2.6 eV) was assigned to the two Type I $\pi^*(s)-v\pi^*$ states of 5^2A and 8^2A . The $5^2A: \pi^*(s)-v\pi^*$ state have a relatively large intensity and can be associated with the lower-energy tail of the lowest band in the experimental spectrum. On the other hand, for the oNA anion, mixing between π^* and σ^* characters in the MOs is quite large, compared to the other isomers. That would come from the hydrogen-bond interaction between the $-NH_2$ and the $-NO_2$ groups due to their short distance. As a result, the lowest valence excited state is the $3^2A: \pi^*(s)-v\sigma^*$ state rather than $\pi^*(s)-v\pi^*$. The shoulder of the lowest peak in the experimental spectrum is assigned to this state, not to $\pi^*(s)-v\pi^*$.

In the NB anion, the main peaks at 465 nm (2.67 eV) and 335 nm (3.70 eV) in the experimental spectrum reasonably corresponded to 2.65 and 3.66 eV in our calculations, which were assigned to $2^2B_1: \pi^*(s)-v\pi^*$ (Type I) and $4^2A_2: \pi-\pi^*_{SOMO}$ (Type II), respectively. For gas-phase experiments, these electronic states of this anion molecule have been revealed [74]. Mock and Grimsrud observed three spectral peaks in the photodetachment experiments [62]. The state at 3.81 eV in their experiments was assigned to $4^2A_2: \pi-\pi^*(s)$ (Type II) at 3.66 eV in our results. Besides these states, we found Type II valence excited states $3^2B_2: n-\pi^*(s)$, $7^2A_1: n-\pi^*(s)$, and $7^2B_1: \pi-\pi^*(s)$ at 3.00, 3.86, and 4.80 eV, respectively.

In the pNA, the most intense peak at 340 nm (3.65 eV) in the experimental spectrum was easily assigned to the $9^2A'': \pi-\pi^*(s)$ (Type II) state. Our calculations also predict other valence excited states in this energy region. The Type II $6^2A'': n-\pi^*(s)$, $15^2A': n-\pi^*(s)$, and $18^2A': \pi-\pi^*(s)$ states were calculated to be at 3.23, 4.06, and 4.72 eV, respectively. For the Type I excitations, we found another valence state $7^2A': \pi^*(s)-v\pi^*$ at 2.75 eV.

In the mNA, we assigned the spectral peaks at 374 nm (3.32 eV) and 323 nm (3.84 eV) to the $11^2A: \pi^*(s)-\pi^*$ (Type I) and the $17^2A: \pi-\pi^*(s)$ (Type II) states, respectively. In the higher-energy region, two Type II $\pi-\pi^*(s)$ states (27^2A and 28^2A) were calculated to be 4.60 and 5.19 eV. One might expect that the peaks at 374 and 323 nm would not be assigned to the Type I and Type II states (11^2A and 17^2A), but to the two Type II states (17^2A and 27^2A). However, the latter assignment would be unlikely considering the similarity to the band assignments for NB and pNA. Two Type II $n-\pi^*(s)$ states (12^2A and 21^2A) were found at 3.65 and 3.88 eV.

In the oNA, the lowest intense peak at 530 nm (2.34 eV) can be assigned to the $8^2A: \pi^*(s)-v\pi^*$ (Type I) state with the non-negligible contribution of the $7^2A: \pi^*(s)-\sigma^*$ state. Thus, this state includes considerable $\pi^*(s)-v\sigma^*$ character and one should be careful in interpreting the excitation natures. The second peak at 386 nm (3.21 eV) can be tentatively assigned to the $16^2A: \pi^*(s)-\pi^*$ state at 3.61 eV. If

this assignment is correct, the higher-energy shoulder of the lowest peak at 22,000 cm^{-1} (~ 2.7 eV) can be attributed to the $11^2A: \pi^*(s)-\pi^*$ state. Another possible assignment of the peak at 25,900 cm^{-1} can be associated with the 11^2A state. However, we cannot definitely conclude which interpretation is correct for this spectral peak at the present stage. In addition, we tentatively assigned the shoulder band in the lowest peak ($\sim 18,000 \text{ cm}^{-1}$) to the $5^2A: \pi^*(s)-\pi^*$ state. The most intense peak at 320 nm (3.87 eV) in the experimental spectrum would be safely assigned to the $19^2A: \pi-\pi^*(s)$ (Type II) excitation considering the excitation energy, oscillator strength, and similarity to the assignments for NB, pNA, and mNA. Other Type II valence excited states were also found in our calculations, $14^2A: n-\pi^*(s)$, $22^2A: n-\pi^*(s)$, $27^2A: \pi-\pi^*(s)$, and $30^2A: \pi-\pi^*(s)$ at 3.32, 3.96, 4.59, and 5.38 eV, respectively. Although the excitation energy of the 14^2A state is very close to that of the second peak (386 nm) in the experimental spectrum, it is unlikely that this peak can be assigned to the $14^2A: n-\pi^*(s)$ state because of discrepancy between the calculated and observed intensities.

7. Summary

Electronic ground and excited states of anion radicals for CN3B, CN4B, TCNQ, NB, pNA, mNA, and oNA and their absorption spectra were accurately studied by the SAC-CI method. The EAs of these molecules were also calculated, and the differences among the target molecules were discussed in terms of the characters for their SOMO as well as the number of the electron-withdrawing terminal groups. The EAs of the target molecules are basically determined by the number of the $-CN$ or $-NO_2$ groups, e.g. $CN4B > CN3B > CN2B > CNB$. However, the very large EA for TCNQ is interpreted by not only the number of the $-CN$ but also the conjugate effect owing to the electron accommodation to the SOMO. This discussion is also true for the extremely large EA for TCNE. Such knowledge obtained in the present study would be useful for the molecular design of new electron acceptor compounds.

The calculated excitation energies reasonably reproduced the corresponding experimental results. According to our calculated results, the character assignments of the experimentally observed states and new unobserved states were proposed. Except for TCNQ, the forbidden (or very low intense) pure valence excitations: $\pi^*(s)-v\pi^*$ were found in near-infrared region. Moreover, these states for the CN3B and CN4B are considered as pure bound states since the corresponding excitation energies were lower than their vertical EAs of anions. Whereas, in the experimental spectra, it is difficult to find and analyse these states due to their very weak intensities, our theoretical calculations were successful to predict the existences of these hidden valence excited states. For oNA, on the other hand, the

corresponding state is rather considered as $\pi^*(s)-v\sigma^*$ due to the large mixing between π^* and σ^* .

For the large intense peaks, roughly speaking, the lower energy bands ($<\sim 25,000\text{ cm}^{-1}$) are assigned to the Type I $\pi^*(s)-\pi^*$ shape resonance states whereas the higher energy bands ($>\sim 25,000\text{ cm}^{-1}$) are due to the Type II $\pi-\pi^*(s)$ Feshbach resonance states, except TCNQ anion for which the lower and higher bands are assigned to the Type II bound and Type I resonance states, respectively. This unique nature in TCNQ is attributed to its very large EA, or the low energy of the SOMO.

Thus, we proposed the character assignments for most of the reported states in the energy region of $<\sim 40,000\text{ cm}^{-1}$, but for a few states, the assignments are still indefinite because of incomplete theoretical reproduction of the experimental excitation energies or band intensities. This problem may be improved by employing the SAC-CI general-*R* method that can handle many-electron excitations such as the Type III processes in Figure 2, and it will be discussed in the next study.

Acknowledgements

The authors thank Mr Nobuo Kawakami for his support to the researches in QCRI. The calculations were mostly done with the computers at Institute of Molecular Science (IMS) computer centre in Okazaki, whom the authors deeply acknowledge.

Disclosure statement

No potential conflict of interest was reported by the authors.

Supplemental data

Supplemental data for this article can be accessed <http://dx.doi.org/10.1080/00268976.2015.1008064>.

References

- [1] H. Akamatu, H. Inokuchi, and Y. Matsunaga, *Nature* **173**, 168 (1954).
- [2] J. Ferraris, D.O. Cowan, V. Walatka, and J.H. Perlstein, *J. Am. Chem. Soc.* **95**, 948 (1973).
- [3] L.B. Coleman, M.J. Cohen, D.J. Sandman, F.G. Yamagishi, A.F. Garito, and A. Heeger, *J. Solid State Commun.* **12**, 1125 (1973).
- [4] D. Jerome, A. Mazaud, M. Ribault, and K. Bechgaard, *J. Phys. Lett.* **41**, 95 (1980).
- [5] E. Collet, M.H. Lemeec-Cailleau, M.B.-L. Cointe, H. Cailleau, M. Wulff, T. Luty, S. Koshihara, M. Meyer, L. Toupet, P. Rabiller, and S. Techert, *Science* **300**, 612 (2003).
- [6] R.S. Potember, T.O. Poehler, and D.O. Cowan, *Appl. Phys. Lett.* **34**, 405 (1979).
- [7] W. Kaim and M. Moscherosch, *Coord. Chem. Rev.* **129**, 157 (1994).
- [8] M.L. Kaplan, R.C. Haddon, F.B. Bramwell, F. Wudl, J.H. Marshall, D.O. Cowan, and S. Gronowitz, *J. Phys. Chem.* **84**, 427 (1980).
- [9] N. Hosaka, M. Obata, M. Suzuki, T. Saiki, and K. Takeda, *Appl. Phys. Lett.* **92**, 113305 (2008).
- [10] Y. Iida, *Bull. Chem. Soc. Jpn.* **42**, 71 (1969).
- [11] P.D. Burrow, A.E. Howard, A.R. Johnston, and K.D. Jordan, *J. Phys. Chem.* **96**, 7570 (1992).
- [12] A.L. Farragher and F.M. Page, *Trans. Faraday Soc.* **63**, 2369 (1967).
- [13] F.M. Page and G.C. Goode, *Negative Ions and the Magnetron* (Wiley-Interscience, New York, 1969).
- [14] C.E. Klots, R.N. Compton, and V.F. Raaen, *J. Chem. Phys.* **60**, 1177 (1974).
- [15] R.N. Compton and C.D. Cooper, *J. Chem. Phys.* **66**, 4325 (1977).
- [16] E.A. Brinkman, E. Gunther, O. Schafer, and J.I. Brauman, *J. Chem. Phys.* **100**, 1840 (1994).
- [17] E. Orti, R. Viruela, and P.M. Viruela, *J. Phys. Chem.* **100**, 6138 (1996).
- [18] B. Milian, R. Pou-Amerigo, R. Viruela, and E. Orti, *Chem. Phys. Lett.* **391**, 148 (2004).
- [19] T. Miyahara and H. Nakatsuji, *The Mechanism of Photo Induced Phase Transition in TTF-TCNE*, preprint.
- [20] T. Tsukuda, T. Kondow, C.E.H. Dessent, C.G. Bailey, M.A. Johnson, J.H. Hendricks, S.A. Lyapustina, and K.H. Bowen, *Chem. Phys. Lett.* **269**, 17 (1997).
- [21] K.D. Jordan and P.D. Burrow, *Acc. Chem. Res.* **11**, 341 (1978).
- [22] R. Zahradnik and P. Carsky, *J. Phys. Chem.* **74**, 1240 (1970).
- [23] T. Shida, *Physical Sciences Data 34 "Electronic Absorption Spectra of Radical Ions"* (Elsevier, Amsterdam, 1988).
- [24] T. Shida and S. Iwata, *J. Phys. Chem.* **75**, 2591 (1971).
- [25] T. Shida and S. Iwata, *J. Chem. Phys.* **56**, 2858 (1972).
- [26] T. Shida and S. Iwata, *J. Am. Chem. Soc.* **95**, 3473 (1973).
- [27] T. Shida, S. Iwata, and M. Imamura, *J. Phys. Chem.* **78**, 741 (1974).
- [28] H. Nakatsuji and K. Hirao, *J. Chem. Phys.* **68**, 2053 (1978).
- [29] H. Nakatsuji, *Chem. Phys. Lett.* **59**, 362 (1978).
- [30] H. Nakatsuji, *Chem. Phys. Lett.* **67**, 329 (1979).
- [31] H. Nakatsuji, in *Computational Chemistry, Reviews of Current Trends*, edited by J. Leszczynski (World Scientific, Singapore, 1997). Vol. 2.
- [32] H. Nakatsuji, J. Hasegawa, and K. Ohkawa, *Chem. Phys. Lett.* **296**, 499 (1998).
- [33] K. Kuramoto, M. Ehara, and H. Nakatsuji, *J. Chem. Phys.* **122**, 014304 (2005).
- [34] K. Fujimoto, J. Hasegawa, S. Hayashi, and H. Nakatsuji, *Chem. Phys. Lett.* **432**, 252 (2006).
- [35] H. Nakatsuji, T. Miyahara, and R. Fukuda, *J. Chem. Phys.* **126**, 084104 (2007).
- [36] J. Hasegawa, K. Fujimoto, B. Swerts, T. Miyahara, and H. Nakatsuji, *J. Comp. Chem.* **28**, 2443 (2007).
- [37] N. Nakatani, J. Hasegawa, and H. Nakatsuji, *J. Am. Chem. Soc.* **129**, 8756 (2007).
- [38] K. Fujimoto, J. Hasegawa, and H. Nakatsuji, *Bull. Chem. Soc. Jpn.* **82**, 1140 (2009).
- [39] R. Cammi, R. Fukuda, M. Ehara, and H. Nakatsuji, *J. Chem. Phys.* **133**, 024104 (2010).
- [40] R. Fukuda and M. Ehara, *J. Chem. Phys.* **137**, 134304 (2012).
- [41] T. Miyahara, H. Nakatsuji, and H. Sugiyama, *J. Phys. Chem. A* **117**, 42 (2013).
- [42] T. Miyahara and H. Nakatsuji, *J. Phys. Chem. A* **117**, 14065 (2013).
- [43] Y. Honda, M. Hada, M. Ehara, and H. Nakatsuji, *J. Phys. Chem. A* **106**, 3838 (2002).
- [44] Y. Honda, M. Hada, M. Ehara, and H. Nakatsuji, *J. Phys. Chem. A* **111**, 2634 (2007).
- [45] H. Nakashima, T. Shida, and H. Nakatsuji, *J. Chem. Phys.* **136**, 214306 (2012).

- [46] Y. Honda, T. Shida, and H. Nakatsuji, *J. Phys. Chem. A* **116**, 11833 (2012).
- [47] M.J. Frisch, G.W. Trucks, H.B. Schlegel, G.E. Scuseria, M.A. Robb, J.R. Cheeseman, G. Scalmani, V. Barone, B. Mennucci, G.A. Petersson, H. Nakatsuji, M. Caricato, X. Li, H.P. Hratchian, A.F. Izmaylov, J. Bloino, G. Zheng, J.L. Sonnenberg, M. Hada, M. Ehara, K. Toyota, R. Fukuda, J. Hasegawa, M. Ishida, T. Nakajima, Y. Honda, O. Kitao, H. Nakai, T. Vreven, J.A. Montgomery, Jr., J.E. Peralta, F. Ogliaro, M. Bearpark, J.J. Heyd, E. Brothers, K.N. Kudin, V.N. Staroverov, T. Keith, R. Kobayashi, J. Normand, K. Raghavachari, A. Rendell, J.C. Burant, S.S. Iyengar, J. Tomasi, M. Cossi, N. Rega, J.M. Millam, M. Klene, J.E. Knox, J.B. Cross, V. Bakken, C. Adamo, J. Jaramillo, R. Gomperts, R.E. Stratmann, O. Yazyev, A.J. Austin, R. Cammi, C. Pomelli, J.W. Ochterski, R.L. Martin, K. Morokuma, V.G. Zakrzewski, G.A. Voth, P. Salvador, J.J. Dannenberg, S. Dapprich, A.D. Daniels, O. Farkas, J.B. Foresman, J.V. Ortiz, J. Cioslowski, and D.J. Fox, *Gaussian 09, Revision B.01* (Gaussian Inc., Wallingford CT, 2010).
- [48] T.H. Dunning, *J. Chem. Phys.* **53**, 2823 (1970).
- [49] T.H. Dunning Jr and P.J. Hay, in *Modern Theoretical Chemistry*, edited by H.F. Schaefer III (Plenum Press, New York, 1977). Vol. 3.
- [50] H. Nakatsuji, *Chem. Phys.* **75**, 425 (1983).
- [51] SAC-CI GUIDE, <http://www.qcri.or.jp/sacci/>
- [52] R. Fukuda and H. Nakatsuji, *J. Chem. Phys.* **128**, 094105 (2008).
- [53] H. Nakatsuji, J. Ushio, and T. Yonezawa, *Can. J. Chem.* **63**, 1857 (1985).
- [54] P.-O. Löwdin, *J. Math. Phys.* **3**, 969 (1962).
- [55] H.S. Taylor, *Adv. Chem. Phys.* **18**, 91 (1970).
- [56] J. Simons and K.D. Jordan, *Chem. Rev.* **87**, 535 (1987).
- [57] C.C. Ballard, M. Hada, and H. Nakatsuji, *Bull. Chem. Soc. Jpn.* **69**, 1901 (1996).
- [58] H. Nakatsuji, *Chem. Phys. Lett.* **177**, 331 (1991).
- [59] M. Ehara, M. Ishida, K. Toyota, and H. Nakatsuji, in *Reviews in Modern Quantum Chemistry*, edited by A tribute to Professor Robert G. Parr, K.D. Sen (World Scientific, Singapore, 2003). pp. 293.
- [60] G.L. Swartz and W.M. Gulick Jr, *Mol. Phys.* **30**, 869 (1975).
- [61] R.P. Mason and J.E. Harriman, *J. Chem. Phys.* **65**, 2274 (1976).
- [62] R.S. Mock and E.P. Grimsrud, *J. Am. Chem. Soc.* **111**, 2861 (1989).
- [63] S. Chowdhury, H. Kishi, G.W. Dillow, and P. Kebarle, *Can. J. Chem.* **67**, 603 (1989).
- [64] P. Kebarle and S. Chowdhury, *Chem. Rev.* **87**, 513 (1987).
- [65] E.C.M. Chen, E.S. Chen, M.S. Milligan, W.E. Wentworth, and J.R. Wiley, *J. Phys. Chem.* **96**, 2385 (1992).
- [66] E.C.M. Chen, J.R. Wiley, C.F. Batten, and W.E. Wentworth, *J. Phys. Chem.* **98**, 88 (1994).
- [67] C. Desfrancois, V. Periquet, S.A. Lyapustina, T.P. Lippa, D.W. Robinson, K.H. Bowen, H. Nonaka, and R.N. Compton, *J. Chem. Phys.* **111**, 4569 (1999).
- [68] C. Huh, C.H. Kang, H.W. Lee, H. Nakamura, M. Mishima, Y. Tsuno, and H. Yamataka, *Bull. Chem. Soc. Jpn.* **72**, 1083 (1999).
- [69] A. Zlatkls, C.K. Lee, W.E. Wentworth, and E.C.M. Chen, *Anal. Chem.* **55**, 1596 (1983).
- [70] S. Chowdhury and P. Kebarle, *J. Am. Chem. Soc.* **108**, 5453 (1986).
- [71] M. Taguchi, Y. Matsumoto, H. Namba, Y. Aoki, and H. Hiratsuka, *Nucl. Instr. Meth. Phys. Res. B* **134**, 427 (1998).
- [72] K. Watanabe, T. Asahi, and H. Masuhara, *J. Phys. Chem.* **100**, 18436 (1996).
- [73] S. Hashimoto, *J. Chem. Soc. Faraday Trans.* **93**, 4401 (1997).
- [74] H.A. Jimenez-Vasquez, M.E. Ochoa, G. Zepeda, A. Modelli, D. Jones, J.A. Mendoza, and J. Tamariz, *J. Phys. Chem. A* **101**, 10082 (1997).